Polymer Chemistry

Accepted Manuscript

ROYAL SOCIETY OF CHEMISTRY

www.rsc.org/polymers

Melt Recrystallization Behavior of Carbon-coated Melt-drawn Oriented Isotactic Polypropylene Thin Films

Le Ma, Jie Zhang, Mushtaque A. Memon, Xiaoli Sun, Huihui Li and Shouke Yan*

State Key Laboratory of Chemical Resource Engineering, Beijing University of Chemical Technology, Beijing 100029, China

To whom all correspondence should be addressed

E-mail: skyan@iccas.ac.cn

Tel. 0086-10-64455928

Fax 0086-10-64455928

ABSTRACT:

The melt recrystallization of vacuum carbon evaporated melt-drawn iPP thin films under varying the melting temperatures, melting times and recrystallization temperatures was studied by means of transmission electron microscopy combined with electron diffraction. It was found that the carbon-coated melt-drawn highly oriented iPP thin films melt-recrystallized always in an oriented way with crystalline lamellae well ordered perpendicular to the drawing direction during sample preparation. This is related to the strong fixing effect of the vacuum evaporated carbon film on the oriented iPP chain stems in the surface layer. Since these fixed iPP chain stems are originally included in the α-iPP crystal lattice, they serve as α-iPP nuclei during the recrystallization process and induce highly oriented iPP lamellae composed of only α-iPP crystals. This indicates that the frequently reported orientation-induced β-iPP crystallization is a nucleation controlled process. Moreover, by comparing the original oriented structure of melt-drawn iPP films with the recrystallized ones, it is concluded that the characteristic wide angle lamellar branching is severely suppressed in elongation-induced crystallization, while takes place evidently during melt-recrystallization.

Keywords: Polypropylene, Recrystallization, Orientation, Polymorphism

1. INTRODUCTION

Isotactic polypropylene (iPP) is one of the most widely studied polymers due to its simple chemical structure and wide applications as conventional plastics. It can crystallize in different crystal structures and morphologies depending on processing condition and molecular parameters, such as the molecular weight, molecular weight distribution and tacticity etc. Up to now, at least three different modifications grown under varied conditions, designated as monoclinic α-form, trigonal (or most frequently hexagonal) β-form and orthorhombic γ-form, have been reported.[1-6] Also a so-called smectic mesophase, which is sometimes referred to as a conformational disordered phase, has been reported.[7, 8] It is well known that the monoclinic α-iPP is the thermodynamically most stable one and can be easily obtained through regular crystallization either from solution or from melt of the commercial grade iPP. The β-form is thermodynamically metastable and can hardly be produced under normal processing conditions. However, the β-iPP exhibits different superior performance, including lower crystal density, lower melting temperature and fusion enthalpy, markedly improved impact strength and toughness.[9-13] Moreover, microporous films, which have been widely applied as gas exchange membranes or separators for lithium batteries, can be prepared by stretching the β-iPP film. Therefore, special techniques were developed for generating β-iPP. The most frequently selected procedure for getting β-iPP is the crystallization under the presence of proper nucleation agents during bulk crystallization.[14-18] Crystallization of sheared or strained iPP melt also encourages the formation of β-iPP.[19-21] Therefore, the origin of the shear or strain induced β-iPP crystallization has drawn due attentions of many research groups.[20-23] It was found that the oriented α-crystals form immediately after shear and then the β-crystals grow subsequently. This suggests that the surface of the oriented α-crystal entities may provide nucleation sites for the growth of β-iPP crystals.

The above mentioned results just provide us some speculations about the formation mechanism of β-iPP crystals from sheared melt. Detailed information about shear-induced β crystallization of iPP has been obtained by fiber pulling procedure, in which the shear-induced crystallization of iPP was performed by pulling the fiber embedded in iPP melt along the fiber axis.[9, 24-26] In this way, a thin layer of the molten iPP matrix in contact with the fiber will be sheared by pulling the fiber. This process is confirmed to be efficient in producing β-iPP crystals. According to the morphological feature at the fiber/matrix interface, it was suggested that β-iPP crystallization is triggered by a αβ transition at the growth front of the shear-induced highly oriented α-iPP row nuclei.[12, 13, 27-29] One thing remaining hard to be understood is about why the αβ transition takes place at the growth front of the α-iPP row nuclei rather than the growth of α-iPP crystals.

To get more insight of the orientation-induced β-iPP crystallization, our research group has utilized an experimental set-up, in which the highly oriented iPP fibers were introduced into their homogeneity molten matrix.[30-35] In this process, the iPP molecular chain or chain segment orientation in the melt was regulated by controlling the melting statues of the iPP fibers. Systematic studies found that partial melting followed by recrystallization of the iPP fibers enables the formation of β-iPP transcrystals in the matrix. The β-iPP crystallization depends on the molecular chain orientation of the iPP in its molten state. It seems that only when the iPP molecular chains or chain segments ordered in an orientation window will crystallize in its β-form.[36] It should be pointed out that, in our experimental procedure, some extent of shear on the iPP matrix could be generated by fiber introduction, even though it does not obviously influence the recrystallization behavior of the iPP. Moreover, it has been confirmed that in the used experimental set up, the matrix iPP was confirmed to be involved in the β-nucleation process through interdiffusion with the oriented chains of molten iPP fiber.[37] To avoid the matrix influence on the β-iPP crystallization, we have recently studied the melt-recrystallization of highly oriented iPP fibers by embedding them into an amorphous matrix of atactic polystyrene by optical microscopy.[38] The results also suggest that certain chain or chain segment orientation of iPP in the molten fiber is required for β-iPP crystallization but a higher orientation of the iPP chains or chain segments encourages the growth of iPP crystals in the α-form. A detailed study using transmission electron microscopy (TEM) on the fiber system is, however, not possible. Considering that the surface carbon-coated highly oriented polymer film can keep its high orientation during melting,[39-47] the present work performed an TEM study of the melt-recrystallization of carbon-coated melt-drawn oriented iPP thin films. The results confirmed that the excellent chain or chain segment orientation can only induce the crystallization of α-iPP.

2 EXPERIMENTAL SECTION

2.1 Material. The iPP used in this study is obtained from Aldrich Chem. America. Its melt flow index is 0.50g/min and the weight average molecular weight is about 5.8×10^5. The peak melting temperature is measured by DSC to be 163 °C.

2.2 Preparation. Highly oriented thin iPP films were prepared according to a melt-draw technique developed by Peterman and Gohil.[48] According to this technique, a small amount of a 0.5 wt% iPP solution in xylene was dispersed uniformly on a preheated glass plate at 140 °C, where the xylene solvent was allowed to evaporate. After evaporation of the solvent, the thin molten iPP layer of ca. 1 μm in thickness was then picked up by a motor-driven cylinder with a drawing speed of about 20 cm/s and highly oriented ultrathin iPP films of ca. 50 nm were collected. The thus prepared iPP thin films were then vacuum carbon deposited on one side and then heat-treated under different conditions, as indicated in the text, for electron microscopy study.

2.3 Characterization. For TEM observation, a JEOL JEM-2100 TEM operated at 200 kV was used in this study. Phase contrast bright field (BF) electron micrographs were obtained by defocus of the objective lens. In order to minimize radiation damage of the crystals by the electron beam, focusing was carried out on an area and the specimen film was then translated to its adjacent undamaged area for recording the images immediately.

3 RESULTS

The microstructures of melt-drawn iPP thin films have been reported in literatures.[37, 38] To make the reading of this paper self-contained, we here present a bright-field phase contrast electron micrograph and its corresponding diffraction pattern of a melt-drawn highly oriented iPP thin film in Figure 1. The arrow in the picture indicates the drawing direction during film preparation. In the defocused phase contrast bright-field image, the bright lines represent the lower density amorphous phase, while the gray ones represent the higher density crystalline lamellae of iPP. We can clearly see that the melt-drawn iPP film consists of highly oriented lamellar structure with the lamellae arranged perpendicular to the drawing direction, demonstrating an alignment of the iPP molecular chains or chain segments along the drawing direction during film preparation. The corresponding electron diffraction result further confirms the high orientation of the melt-drawn iPP thin film with the molecular chains aligned in the film plane and along the drawing direction. All of the sharp and well defined reflection spots on the electron diffraction pattern are accounted for by a monoclinic unit cell with parameters a = 0.666 nm, b = 2.078 nm, c = 0.6495 nm, and β= 99.62º. This demonstrates that the melt-drawn iPP film consists of the α-form edge-on lamellar crystals. Furthermore, the coexistence strong (110) reflection spots on equator direction and very weak (110) reflection spots on the meridian direction (hardly discernable) reveals that the characteristic lamellar branching of the α-iPP is not pronounced in elongation-induced crystallization with respect to the bulk crystallization.

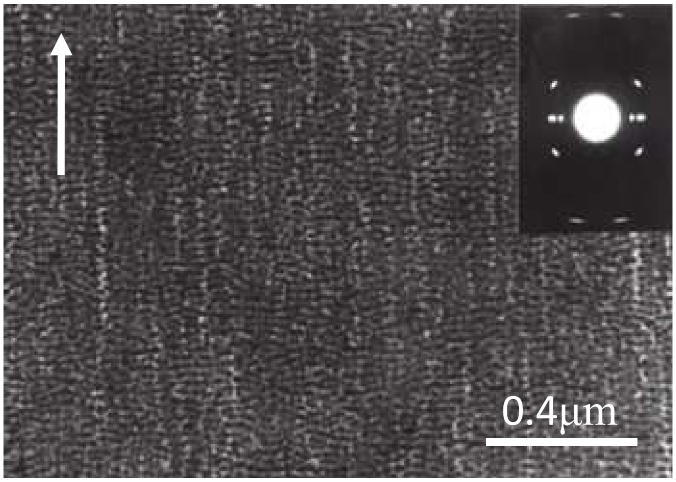

Figure 1. A BF electron micrograph and its corresponding electron diffraction pattern (inset, in proper relative orientation) of a melt-drawn iPP thin film. The arrow in the picture indicates the drawing direction of the film during preparation

Figure 2 shows the BF electron micrograph and its corresponding electron diffraction pattern of a melt-drawn iPP thin film supported by an amorphous carbon layer, i.e., placed on a pre-formed carbon film, and isothermally recrystallized at 120 °C for 2h after heat-treated at 180 °C for 5 min. From the BF image, Figure 2a, we can see that the original oriented lamellar structure disappears. The iPP recrystallized in lathlike microcrystal form. The corresponding electron diffraction pattern, Figure 2b, shows still well defined reflection spots. These electron diffraction spots are confirmed to be the (*hk*0) reflections of the monoclinic α-iPP crystals. This indicates that the crystallographic *c*-axes of the iPP crystals in the melt recrystallized film are vertical to the film plane, i.e., the formation of flat-on lathlike lamellae. This demonstrates that, during melt-recrystallization process, there is no memory effect of the pre-oriented iPP molecular chains included in the oriented α-iPP crystals.

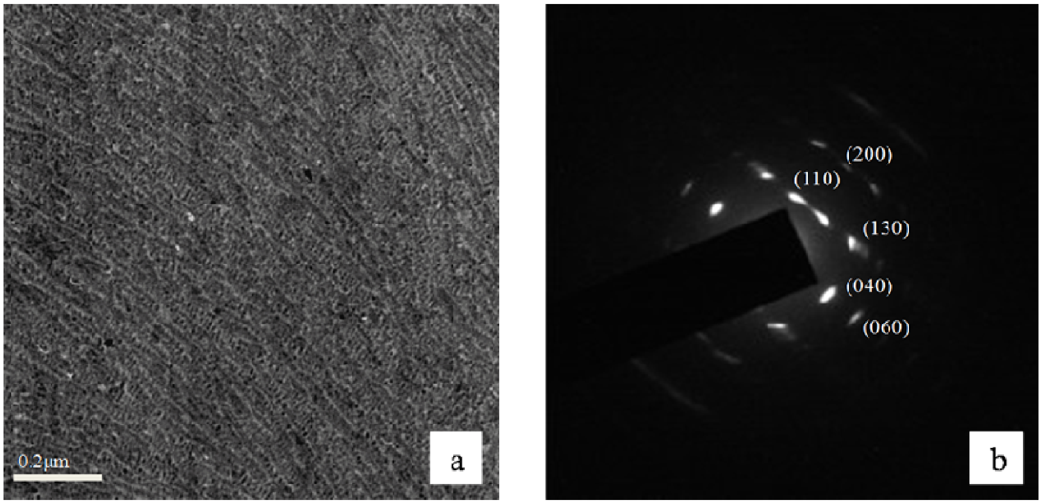

Figure 2. BF electron micrograph (a) and its corresponding electron diffraction pattern (b) of a carbon layer supported melt-drawn iPP thin film, which has been heat-treated at 180 °C for 5 min and then isothermally crystallized at 120 °C for 2h.

It was found that the melt recrystallization behavior of vacuum carbon deposited melt-drawn iPP films is totally different from the carbon film supported ones. Figure 3 shows the BF electron micrograph and its corresponding electron diffraction pattern of a carbon-coated melt-drawn iPP thin film, which has been heat-treated at 180 °C for 5 min and then isothermally recrystallized at 120 °C for 2h. From the BF microimage, Figure 3a, we see predominant edge-on lamellae aligned mostly perpendicular to the drawing direction of the sample during preparation. Few lamellae arranging approximately in the direction of stretching are also observed. This is associated with the characteristic wide angle lamellar branching of the α-iPP, which is further confirmed by the appearance of the strong (110) reflection spots along the drawing direction during film preparation, Figure 3b. The corresponding electron diffraction pattern shows again sharp and well defined reflection spots similar to the pristine melt-drawn iPP film. This means that the coated carbon layer has preserved the molecular chain orientation of the melt-drawn iPP film and enables an oriented melt recrystallization of iPP. The appearance of only α-iPP diffractions tells us that the recrystallized well ordered iPP lamellae are also composed of only α-iPP crystals. This is different from the melt recrystallization of highly oriented iPP fibers embedded in the atactic polystyrene matrix, where β-iPP crystals are frequently observed after melt at 180 °C and then isothermally recrystallized at temperatures within 100 ~ 140 °C.[38] It should be pointed out that the β-iPP recrystallization of highly oriented iPP fibers is melting status and crystallization condition related. To check whether the different crystallization behavior of carbon-coated melt-drawn iPP films with respect to that of the iPP fibers is caused by melting and recrystallization conditions, recrystallization behavior of carbon-coated melt-drawn iPP films under varied melting temperature, melting time and recrystallization temperature was followed.

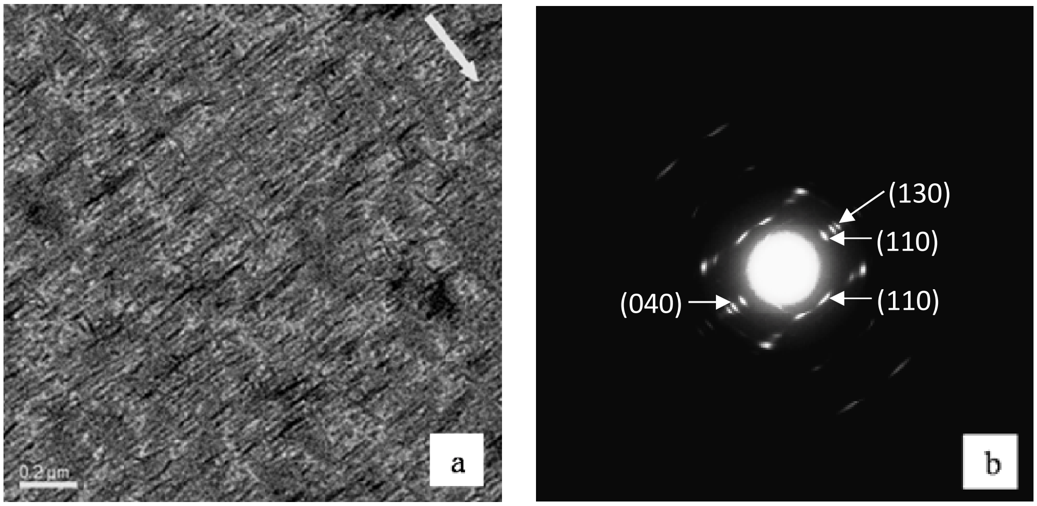

Figure 3. A BF electron micrograph (a) and its corresponding electron diffraction pattern in proper relative orientation (b) of a vacuum carbon evaporated melt-drawn iPP thin film, which has been heat-treated at 180 °C for 5 min and then isothermally crystallized at 120 °C for 2h .The arrow in the picture indicates the drawing direction of the film during preparation.

It was found that the melting temperature does essentially not influence the recrystallization behavior of iPP very much. As examples, Figure 4 shows the BF electron micrographs and their corresponding electron diffraction patterns of the vacuum carbon evaporated melt-drawn iPP thin films, which have been heat-treated at 163 °C and 200 °C for 5 min, respectively, and then cooled to 120 °C for complete isothermal crystallization. It is obvious that the orientation of melt-drawn iPP films is still preserved in both cases. For the sample molten at 163 °C for 5 min, Figures 4a and 4b, even though no branched lamellae can be observed in the BF microimage, the intensity increase of the (110) diffractions along the molecular chain direction (compare the diffraction patterns shown in Figure 4b with the inset of Figure 1) demonstrates the occurrence of melt recrystallization, at least to some extent. For the sample molten at 200 °C for 5 min, Figures 4c and 4d, the well ordered lamellar structure suggests that the carbon coating keeps the high orientation of some iPP chain stems previously included in the crystal lattice during melting at 200 °C. It is these oriented molecular chains or chain segments that in turn serve as nucleation precursors and initiate the oriented crystallization of the molten iPP during cooling. This is different from the melt recrystallization of the amorphous matrix embedded iPP fibers, which will lose orientation after recrystallization by melting at 200 °C. Furthermore, it was confirmed that the reflections in both diffraction patterns are accounted for by the monoclinic unit cell, demonstrating the formation of oriented α-iPP lamellar crystals. It should be mentioned here that the different morphologies observed for the sample molten at different temperatures may be related to the different melting status of the oriented iPP film. At lower melting temperature, a complete relaxation of the iPP molecular chains in the highly oriented thin film is not expected, which influences the recrystallization behavior of iPP and producing a slightly different lamellar arrangement.

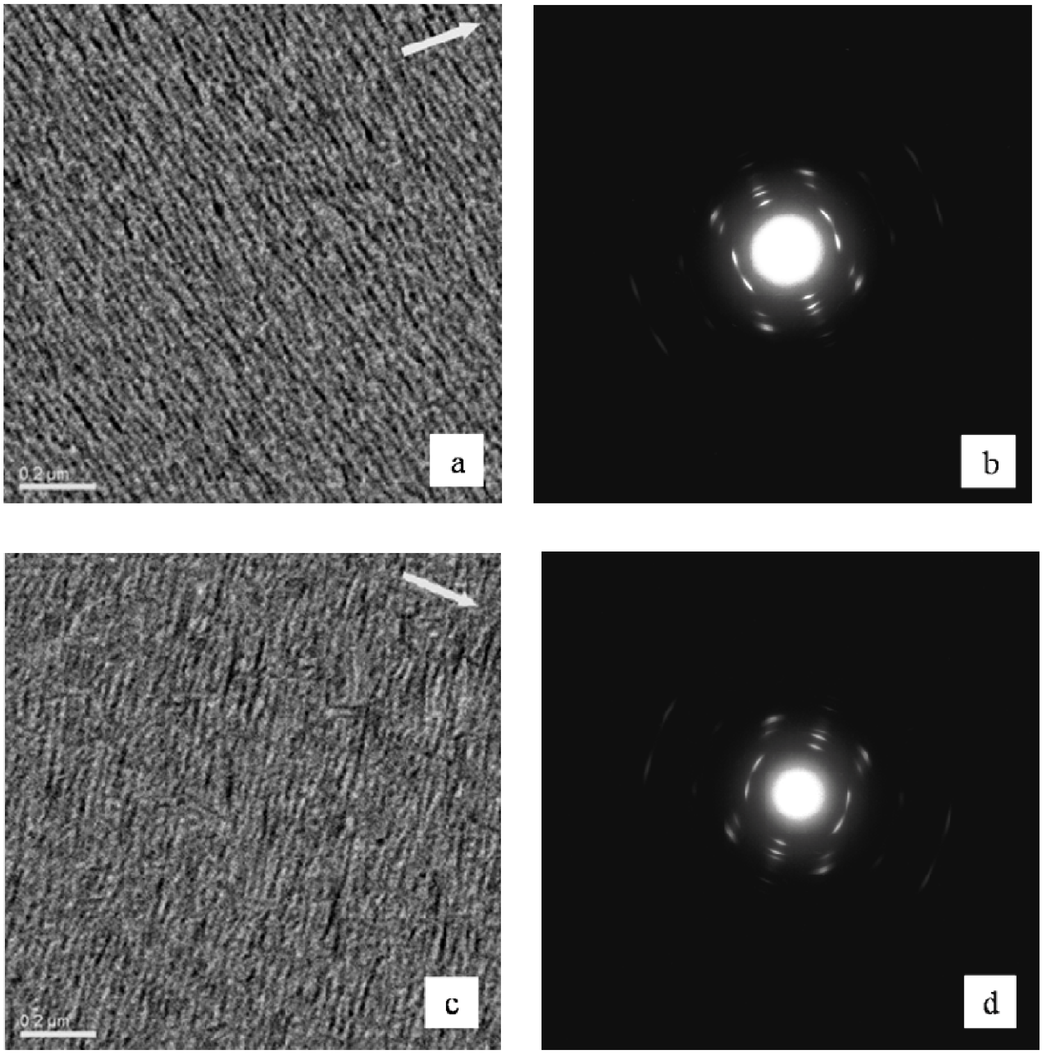

Figure 4. BF electron micrographs (a and c) and the corresponding electron diffraction patterns (b and d) of the vacuum carbon evaporated melt-drawn iPP thin films, which have been heat-treated at 163 °C (a and b) and 200 °C (c and d) for 5 min, respectively, and then isothermally crystallized at 120 °C for 2h.The arrows in the pictures indicate the drawing direction of the films during preparation.

The above experimental results demonstrated that the melting temperature does not influence the recrystallization behavior of the carbon-coated melt-drawn iPP thin films very much. They always recrystallize in highly oriented α-iPP crystals. It was further found that the melting duration at all melting temperatures exhibits also no evident effect on the recrystallization behavior of the carbon-coated melt-drawn iPP thin films. Figure 5 shows two representative examples with the vacuum carbon evaporated melt-drawn iPP thin films molten at 200 °C for 30 min and 60 min, respectively, and then isothermally crystallized at 120 °C for 2h. The bright field images display still highly oriented edge-on iPP lamellae arranged perpendicular to the original drawing direction. The electron diffraction results demonstrate that all of the highly oriented lamellar crystals are composed α-iPP.

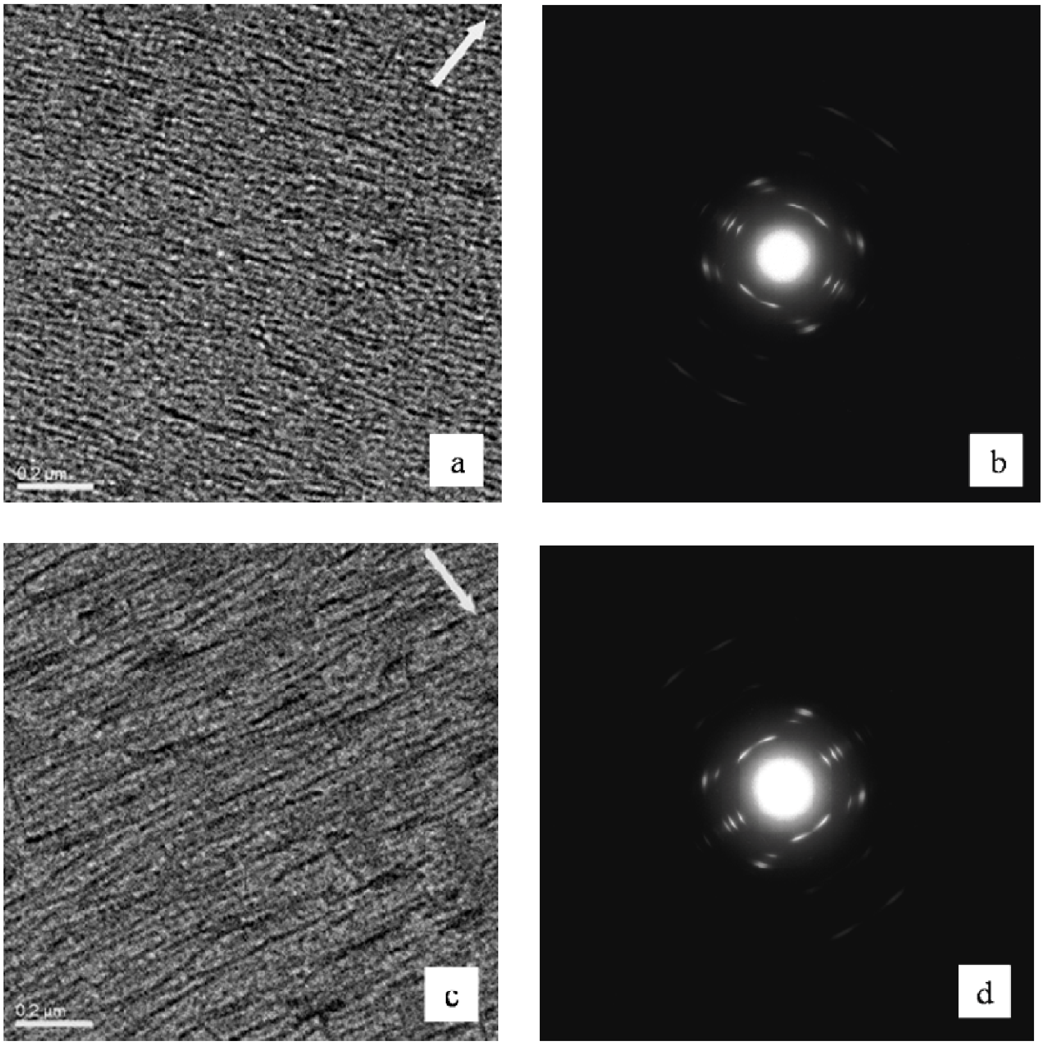

Figure 5. BF electron micrographs (a and c) and the corresponding electron diffraction patterns (b and d) of the vacuum carbon evaporated melt-drawn iPP thin films, which have been heat-treated at 200 °C for 30 min (a and b) and 60 min (c and d), respectively, and then isothermally crystallized at 120 °C for 2h. The arrows in the pictures indicate the drawing direction of the film during preparation.

Through systematic studies, Varga et al. proposed that the β-iPP crystallization of the sheared iPP melt by fiber pulling is triggered by a α to β growth transition occurred at the growth front of the α-row nuclei. It was suggested that a higher growth rate of the β-phase than that of α-phase is the kinetic requirement for the αβ-growth transition.[13, 19, 27, 49] This can be achieved only in a certain crystallization temperature range of 100 ~ 140 °C. Even though the crystallization temperature of 120 °C in all of the aforementioned experiments falls in the above mentioned temperature window, we have further checked whether the oriented α-iPP recrystallization in all cases is affected by crystallization temperature or not. Through chosen several crystallization temperatures in the range of 100 ~ 140 °C, such as 100 °C, 110 °C, 130 °C, 140 °C, we found that highly oriented α-iPP lamellar crystals were always observed after recrystallization under any melting condition used. As examples, Figure 6 shows the bright field electron micrographs and their corresponding diffraction patterns of the vacuum carbon evaporated melt-drawn iPP thin films heat-treated at 200 °C for 5 min and then recrystallized at 110 °C and 130 °C respectively.

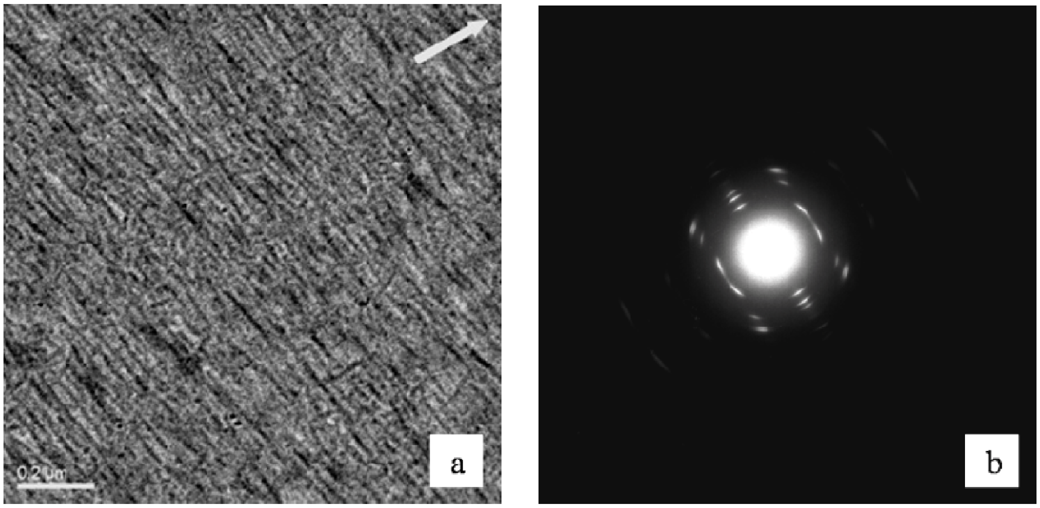

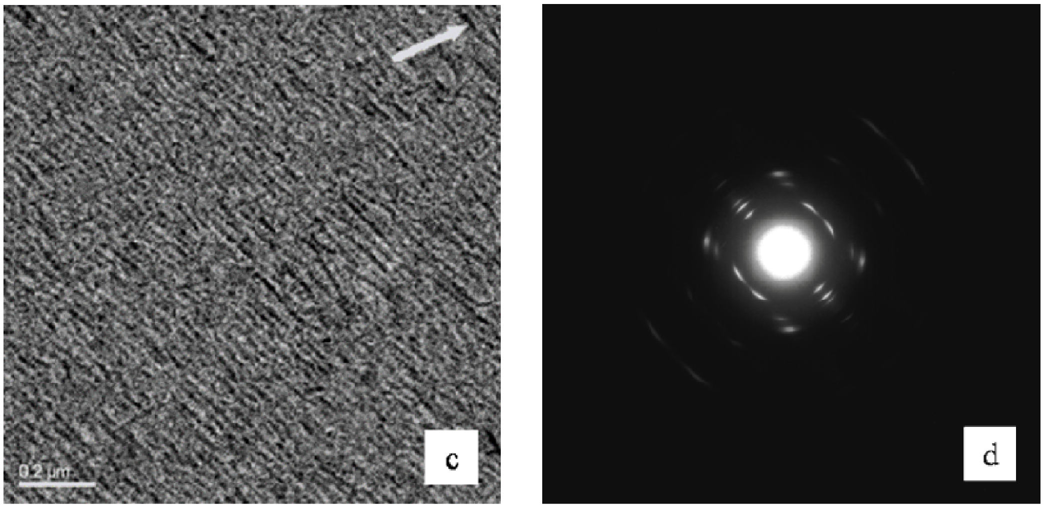

Figure 6. BF electron micrographs (a and c) and the corresponding electron diffraction patterns (b and d) of the vacuum carbon evaporated melt-drawn iPP thin films, which have been heat-treated at 200 °C for 5 min and then isothermally crystallized at 110 °C (a and b) and 130 °C (c and d) for 2h, respectively. The arrows in the pictures indicate the drawing direction of the film during preparation.

4 DISCUSSION

According to the above obtained experimental results, it is clear that a thin vacuum coated carbon layer on the highly oriented iPP thin films results in an oriented melt-recrystallization of them in the α-form under any thermal treatment and crystallization conditions. This is different from the melt-recrystallization of highly oriented iPP fibers embedded either in its single polymer melt or in an amorphous polystyrene matrix, where (i) the recrystallized iPP fibers lose their orientation when melting was performed at temperatures above 200 °C and (ii) β-iPP crystals were frequently observed under suitable heat-treatment and crystallization temperatures. In the next section, the origin of the oriented α-iPP recrystallization of carbon-coated pre-oriented iPP thin films will be discussed.

Let us first discuss the oriented melt-recrystallization of the carbon-coated highly oriented iPP thin films. Studies on the melt-recrystallization behavior of the carbon-coated highly oriented PE thin films suggests that the vacuum evaporated carbon layer has strong fixing effect on the surface monolayer molecules of the well ordered thin PE films and prevented the extended crystalline macromolecular chain stems previously arranged in the crystals from relaxing during melting.[41] Raman spectroscopy results suggest the formation of new carbon-carbon bonds of the carbon-coated PE film, resulting in some of the PE chain stems are fixed to the coated carbon layer via covalent bond.[47] It is this bonding effect that retards the relaxation of the PE chains at the spot and, therefore, preserves the original orientation of the PE stems at high temperature. The extended macromolecular chain stems act as the nucleation sites during the recrystallization process and, therefore, enable the oriented re-growth of the PE melts. This oriented recrystallization mechanism of PE films may also valid to the iPP oriented thin films. The oriented recrystallization behavior of iPP is, however, somewhat different from the PE. This originates from the characteristic wide angle lamellar branching of iPP. For the as prepared highly oriented iPP thin films, the elongation of the iPP melt during stretching leads to a high orientation of the molecular chains or chain segments. The highly oriented iPP chains or chain segments trigger an oriented crystallization of iPP in well ordered lamellar structure with molecular chains preferentially oriented in the stretching direction, as presented in Figure 7a. During the crystallization of the highly stretched iPP melt, the wide angle lamellar branching has been remarkably suppressed, as judged by the very weak (110) reflection located in the stretching direction (see inset of Figure 1). During the melting process, while some of the iPP molecular chain stems in surface layer are fixed by the carbon layer, most of the iPP molecular chains are relaxed. By recrystallization, the fixed iPP molecular chain stems serve as nuclei and initiate an oriented recrystallization. At the same time, the wide angle lamellar branching takes place for the relaxed iPP molecular chains, as shown in Figure 7b, leading to the appearance of strong (110) reflections in the drawing direction of the original sample.

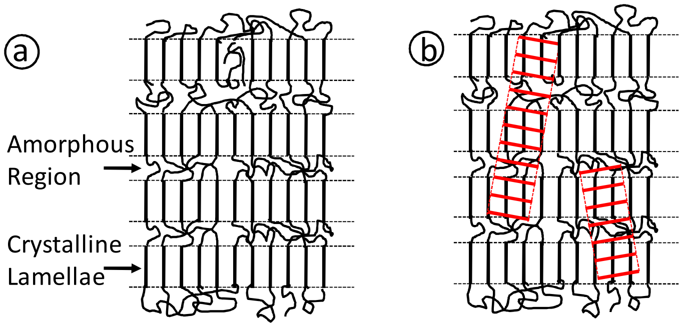

Figure 7 Schematic representation of the oriented structures of carbon coated melt-drawn iPP thin films before (a) and after (b) melt-recrystallization. The drawing direction during film preparation is vertical.

The above discussion has explained why the carbon-coated pre-oriented iPP thin films recrystallize again in oriented structure. Here we will discuss about the oriented α-iPP recrystallization behavior. As mentioned in the introduction part, it was well documented that sheared or elongated iPP melts encourage the β-iPP crystallization. In the melt-draw process, the iPP supercooled melt suffers a high elongation before crystallization. It crystallizes, however, in the α-form. This supports our previous speculation that high chain or chain segment orientation does not favor the crystallization of iPP in β-form. Moreover, the melt-recrystallization of highly oriented iPP fibers embedded in the atactic polystyrene matrix shows that β-iPP crystallization takes place quite frequently under proper melting and recrystallization conditions. It was confirmed that the β-iPP crystallization is a nucleation controlled process. There seems a chain or chain segment orientation window, in which the β-iPP nucleation is most favorable. The present experimental results may support this hypothesis. This can be understood in the following way. A complete melting of the iPP fibers leads to fully relaxation of the iPP molecular chains and formation of random coiled iPP melt. The subsequent recrystallization then proceeds like the normal bulk crystallization and results in the formation of non-oriented α-iPP crystals. If the iPP fibers were not complete molten, the highly oriented iPP molecular chains would relaxed only to some extent. In other words, oriented molecular chains previously included in the highly oriented crystals has been preserved. These ordered molecular chains or chain segments are able to transform into oriented crystalline nuclei and initiate the oriented recrystallization of iPP like the sheared melts of iPP, which encourages the formation of β-iPP crystals depending on chain orientation status. For the carbon-coated iPP melt-drawn thin films, some of the iPP molecular chain stems in surface layer are strongly fixed by the carbon layer during melting, while the rest of the molecular chains will relax completely. The fixed chain stems are originally packed in the α-iPP crystals and will therefore serve as α-iPP nuclei initiating the oriented α-iPP crystallization of the relaxed iPP melt. This has a close resemblance with a phenomenon recently reported by Ann-Kristin Löhmann, Thomas Henze, and Thomas Thurn-Albrecht et al.[50] They found that in the polymer melt contacted with a solid substrate, pre-freezing of polymer chains at the melt–solid interface before crystallization takes place. These pre-freezing of polymer chains are stable above the bulk melting temperature. It is this ordered layer that initiates crystal growth into the bulk and leads to an oriented, homogeneous semicrystalline structure. Taking this into account, oriented recrystallization of carbon-coated highly oriented melt-drawn iPP in its α-form is highly expected.

5 CONCLUSION

The melt recrystallization of vacuum carbon deposited highly oriented iPP thin film was studied by means of transmission electron microscopy combined with electron diffraction. The obtained results indicate that highly oriented lamellar structures of the iPP film are always observed after melting at different temperature for different times and recrystallized under varied temperatures.

This confirms the existence of strong fixing effect of vacuum evaporated thin carbon film on the oriented iPP surface layer, which prevents the iPP molecular chains or chain segments in surface layer from relaxation. It is these fixed chain stems that enable an oriented recrystallization. The oriented iPP lamellae are confirmed to be composed only of α-iPP crystals. This is different from the melt recrystallization behavior of the atactic polystyrene embedded iPP fibers, where β-iPP crystallization occurs most frequently under certain thermal treatment conditions, and is associated to the fixed iPP chain stems. Taking into account that the fixed iPP chain stems are previously included in the α-iPP crystals, they should serve as α-iPP nuclei and initiate the α-iPP recrystallization. This result demonstrates that the orientation-induced β-iPP crystallization is a nucleation controlled process. Moreover, the present results also demonstrate that the characteristic wide angle lamellar branching of iPP is remarkably suppressed in crystallization of elongated iPP melt. It happens, however, during the recrystallization process as judged from the obvious cross-hatched structure of iPP originating from wide angle lamellar branching.

6 Acknowledgements

The financial supports of the National Natural Science Foundations of China (No. 21274009, 21434002 and 51221002) and the program of Introducing Talents of Discipline to Universities (B08003) are gratefully acknowledged.

REFERENCE

(1) H. D. Keith, F. J. Padden, N. M. Walter and H. W. Wyckoff, *J. Appl. Phys.*, 1959, **30**, 1485-1488.

(2) A. Turner-Jones and A. J. Cobbold, *J. Polym. Sci.*, 1968, **6**, 539-546.

(3) F. J. Padden and H. D. Keith, *J. Appl. Phys.*, 1959, **30**, 1479-1484.

(4) B. Lotz, J. C. Wittmann and A. J. Lovinger, *Polymer*, 1996, **37**, 4979-4992.

(5) D. R. Norton and A. Keller, *Polymer*, 1985, **26**, 704-716.

(6) A. J. Lovinger, J. O. Chua and C. C. Gryte, *J. Polym. Sci., Part B: Polym. Phys.*, 1977, **15**, 641-656.

(7) B. Wunderlich, *Thermal analysis*, Academic Press, London, 1990, **Vol.95**, p32.

(8) S. Piccarolo, M. Saiu, V. Brucato and G. Titomanlio, *J. Appl. Polym. Sci.*, 1992, **46**, 625-634.

(9) J. Varga, *J. Macromol. Sci., Part B: Phys.*, 2002, **41**, 1121-1171.

(10) J. Karger-Kocsis, E. Moos, I. Mudra and J. Varga, *J. Macromol. Sci., Part B: Phys.*, 1999, **38**, 647-662.

(11) J. Karger-Kocsis, *Polym. Eng. Sci.*, 1996, **36**, 203-210.

(12) L. Cao, D. Su, Z. Su and X. Chen, *Chin. J. Polym. Sci.*, 2014, **32**, 1167-1175.

(13) Q. Liu, H. Li and S. Yan, *Chin. J. Polym. Sci.*, 2014, **32**, 509-518.

(14) J. Varga, Crystallization, Melting and Supermolecular Structure of Isotactic Polypropylene. In *Polypropylene*: *Structure, Blends and Composites*, J. Karger-Kocsis, Ed.; Chapman & Hall: London, 1995, **Vol. 1**, pp 56-115.

(15) G. Shi, X. Zhang and Z. Qiu, *Makromol. Chem.*, 1992, **193**, 583-591.

(16) M. Dong, Z. Guo, J. Yu and Z. Su, *J. Polym. Sci. Part B: Polym. Phys.,* 2008, **46**, 1725–1733.

(17) M. Dong, Z. Guo, J. Yu and Z. Su, *J. Polym. Sci. Part B: Polym. Phys.,* 2009, **47**, 314–325.

(18) Z. Su, M. Dong, Z. Guo and J. Yu, *Macromolecules,* 2007, **40**, 4217-4224.

(19) E. Devaux and B. Chabert, *Polym. Commun.*, 1991, **32**, 464-468.

(20) J. Varga and J. Karger-Kocsis, *J. Polym. Sci., Part B: Polym. Phys.*, 1996, **34**, 657-670.

(21) J. Varga and G. W. Ehrenstein, *Polymer*, 1996, **37**, 5959-5963.

(22) R. H. Somani, I. Sics and B. S. Hsiao, *J. Polym. Sci., Part B: Polym. Phys.*, 2006, **44**, 3553-3570.

(23) H. Huo, S. Jiang and L. An, *Macromolecules*, 2004, **37**, 2478-2483.

(24) C. Zhang, H. Hu, X. Wang, Y. Yao, X. Dong, D. Wang, Z. Wang and C. Han, *Polymer*, 2007, **48**, 1105-1115.

(25) R. H. Somani, B. S. Hsiao, A. Nogales, H. Fruitwala, S. Srinivas and A. H. Tsou, *Macromolecules*, 2001, **34**, 5902-5909.

(26) J. Varga and J. Karger-Kocsis, *Polym. Bull.*, 1993, **30**, 105-110.

(27) J. Varga and J. Karger-Kocsis, *J. Mater. Sci. Lett.*, 1994, **13**, 1069-1071.

(28) J. Varga and J. Karger-Kocsis, *Polymer*, 1995, **36**, 4877-4881.

(29) J. Varga, *J. Mater. Sci.*, 1992, **27**, 2557-2579.

(30) H. Li, S. Jiang, J. Wang, D. Wang and S. Yan, *Macromolecules*, 2003, **36**, 2802-2807.

(31) H. Li, X. Zhang, X. Kuang, J. Wang, D. Wang, L. Li and S. Yan, *Macromolecules*, 2004, **37**, 2847-2853.

(32) X. Sun, H. Li, X. Zhang, J. Wang, D. Wang and S. Yan, *Macromolecules*, 2006, **39**, 1087-1092.

(33) H. Li, X. Zhang, Y. Duan, D. Wang, L. Li and S. Yan, *Polymer*, 2004, **45**, 8059-8065.

(34) H. Li, J. Liu, D. Wang and S. Yan, *Colloid Polym. Sci.*, 2003, **281**, 973-979.

(35) Q. Liu, X. Sun, H. Li and S. Yan, *Polymer*, 2013, **54**, 4404-4421.

(36) X. Sun, H. Li, J. Wang and S. Yan, *Macromolecules*, 2006, **39**, 8720-8726.

(37) X. Sun, H. Li, X. Zhang, D. Wang, J. M. Schultz and S. Yan, *Macromolecules*, 2010, **43**, 561-564.

(38) L. Ye, H. Li, Z. Qiu and S. Yan, *Phys. Chem. Chem. Phys.*, 2015, **17**, 7576-7580.

(39) S. Yan, F. Katzenberg and J. Petermann, *J. Polym. Sci., Phys. Ed.*, 1999, **37**,1893-1898.

(40) S. Yan and J. Petermann, *Polymer*, 2000, **41**, 6679-6681.

(41) S. Yan, I. Lieberwirth, F. Katzenberg and J. Petermann, *J. Macromol. Sci., Part B: Phys.*, 2003, **B42**, 641-652.

(42) J. Wang, H. Li, J. Liu, Y. Duan, S. Jiang and S. Yan, *J. Am. Chem. Soc.*, 2003, **125**, 1496-1497.

(43) S. Yan, *Macromolecules*, 2003, **36**, 339-345.

(44) N. Taniguchi and A. Kawaguchi, *Macromolecules*, 2005, **38**, 4761-4768.

(45) J. Liu, H. Li, Y. Duan, S. Jiang, Z. Miao, J. Wang, D. Wang and S. Yan, *Polymer*, 2003, **44**, 5423-5428.

(46) K. Lü and D. Yang, *Macromol. Rapid Commun.*, 2005, **26**, 1159-1162.

(47) H. Chang, Q. Guo, D. Shen, L. Li, Z. Qiu, F. Wang and S. Yan, *J. Phys. Chem. B*, 2010, **114**, 13104-13109.

(48) J. Petermann and R. M. Gohil, *J. Mater. Sci.*, 1979, **14**, 2260-2264.

(49) J. Varga, Y. Fujiwara and A. Ille, *Periodica Polytech. Chem. Eng.*, 1990, **34**, 255-271.

(50) A. Löhmann, T. Henze, and T. Thurn-Albrecht, *PNAS*, **111**, 17368–17372.

	Melt Recrystallization Behavior of Carbon-Coated Melt-drawn Oriented Isotactic Polypropylene Thin Films Le Ma, Jie Zhang, Mushtaque A. Memon, Xiaoli Sun, Huihui Li and Shouke Yan*